Numerical Analysis of In-vessel Retention using MARS-Ga for APR 1400 under the gallium-water External Reactor Vessel Cooling System

Sarah Kang [a], Seong Dae Park [a], In Guk Kim[a], In Cheol Bang [a*]
[a]*School of Mechanical and Nuclear Engineering Ulsan National Institute of Science and Technology (UNIST)*
50 UNIST-gil, Ulsan, Republic of Korea 689-798
[*]*Corresponding author: icbang@unist.ac.kr*

1. Introduction

For confirming the feasibility of the gallium-water IVR-ERVCS (In-Vessel Retention of molten corium by external reactor vessel cooling system), this research focuses on the numerical simulation for severe accidents in APR 1400 using MARS-Ga. In this system, the generated decay heat is transferred to liquid gallium through the reactor pressure vessel and then removed from the water pool as an ultimate heat sink. The numerical analyses results show that the temperature range of the liquid gallium is much lower than its boiling point and the natural convection can be confirmed. Because liquid gallium does not have the phase change unlike water, the gallium-water IVR-ERVCS can provide the stable and reliable cooling capability. To solve the limitation of IVR-ERVCS on the critical heat flux and ensure the sufficient thermal margin, it is confirmed that the gallium-water IVR-ERVCS can be a successful severe accident mitigation strategy in nuclear power plants.

2. Methods

2.1 Gallium-water IVR-ERVCS

Fig. 1 shows the advanced illustration of the side cooling concept that two fluids were separated by the block structure [1]. Compared to the current systems, the block structure to divide the region between gallium and water was added like second vessel or liquid metal catcher. Insulation of reactor vessel was also used to reduce the heat loss during normal operation between the reactor vessel and structure instead of the cavity wall. Gallium will be flooded into so-called liquid metal catcher by gravity. The decay heat generated in corium is transferred to liquid gallium through reactor pressure vessel and then to water pool via liquid metal catcher as an ultimate heat sink.

2.2 MARS-Ga modeling

The properties of gallium in MARS-LMR code were generated by using the soft-sphere model based on

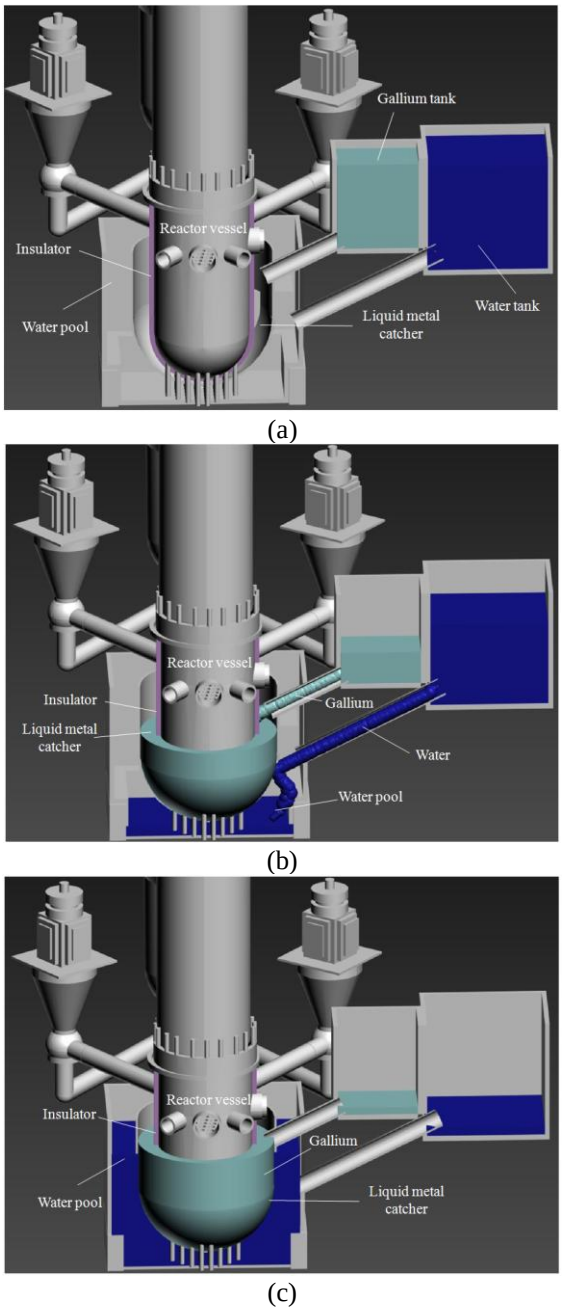

Fig. 1. Illustration of the gallium-water IVR-ERVCS

Monte Carlo calculations for particles interacting with pair potentials [2] and these properties were newly added to MARS-LMR code, MARS-Ga which is applicable for gallium-cooled systems [3]. Numerical analyses of the gallium-water IVR-ERVCS in APR 1400 using MARS-Ga code were performed. Fig. 2 shows the comparison of reactor vessel cavity arrangement of APR 1400 and nodalization of the existing and the gallium-water IVR-ERVCS. The dimension between the insulator and structure (SV253-SV305) refers to CFD geometry of Park and Bang [1]. Table I indicates the initial conditions used in MARS-Ga analysis as well as geometry information. It is assumed that the initial temperature of liquid gallium was water are 313.15 K (40°C). The stainless steel was selected as the material of structure between liquid gallium and water. In schematic of nodalization, flow path of liquid gallium between not only the reactor pressure vessel and the insulator (SV100-SV179) but also the insulator and the structure (SV277-SV305) were composed of single volumes (SV). The water pool was also composed of single volumes from SV579 to SV637. TDV801 is the time-dependent volume (TDV) that vents the generated steam from the water pool. The flow path of liquid gallium and borated water pool were connected with single junctions having a cross flow. In this research, the medium break loss of coolant accident (MBLOCA) of 4.28" break size of the cold leg without actuation of the safety injection pumps, whereas, the safety injection tank (SIT) were actuated effectively have been simulated from the transient

Table I: Geometry of APR 1400 and initial conditions used in MARS-Ga analysis

Geometry and initial condition	Value	
Height [m]	7.4	
Radius of reactor vessel [m]	2.574	
Thickness of reactor vessel [m]	0.165	
Thickness of insulator [m]	0.114	
Thickness of barrier [m]	0.05	
Material of barrier of liquid-metal catcher	Stainless steel	
Initial temperature of gallium [K]	313.15 (40°C)	
Initial temperature of H_2O [K]	313.15 (40°C)	
Total amount of gallium [ton]	704	
Total amount of H_2O [ton]	180	
Heat flux under MBLOCA [MW/m^2]	30°	0.45
	50°	0.85
	70°	1.3
	90°	2.2

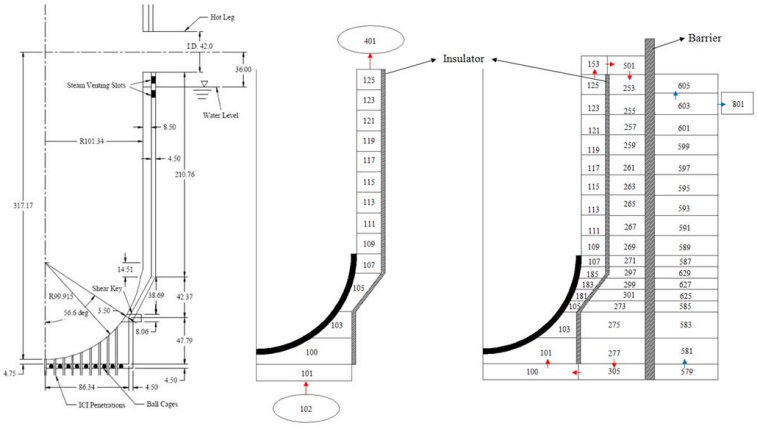

(a) (b) (c)

Fig. 2. Geometry comparison of (a) schematic of APR 1400 reactor vessel and insulator (Unit:inch) [5]; (b) nodalization of the existing IVR-ERVCS, and (c) the current IVR-ERVCS

initiation to reactor vessel failure [4-5]. At the initial stage, the decay heat increases to 2200KW/m^2 in 20s.

3. Results and Discussion

3.1 Temperature distribution of APR 1400 under MBLOCA

The analysis was focused on the range of temperature for outer reactor pressure vessel wall and liquid gallium. The surface temperature distribution of reactor vessel is as shown in fig. 3. As shown in fig. 3, the initial temperature of reactor vessel reaches about from 322.15 K (49°C) to 340.15 K (67°C) and the temperature after heat removal for 3.8hrs, was in the range of 448.15 K (175°C) to 565.15 K (292°C). In the fig. 4, the initial temperature range of liquid gallium is about 313.15 K (40°C) and after 3.8hrs that of liquid gallium is from 373.15 K (100°C) to 402.15 K (129°C). It is found that the maximum temperature of the liquid gallium in cavity is below the boiling point of gallium. The natural convection flow can be confirmed in the gallium and water analysis region. Although the results using MARS-Ga code have the lower value compared to Park and Bang [1], the temperature range was in a good agreement. At the same geometry, the simulation of the water-water IVR-ERVCS was also performed as shown in fig. 3 and 4. The surface temperature distribution of reactor vessel of water-water IVR-ERVCS is slightly lower than that of the gallium-water IVR-ERVCS. Because the specific heat of the liquid gallium is lower than that of the water, the range of the temperature of liquid gallium is higher than that of the water. Additionally the mass flowrate of gallium-water and water-water IVR-ERVCS can be confirmed as shown in fig. 5. Because the gallium-water IVR-ERVCS does not include phase change phenomena, the

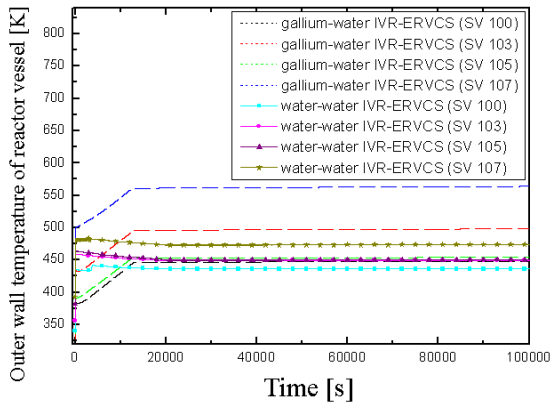

Fig. 3 Wall temperature distribution of outer reactor vessel of the gallium-water and water-water IVR-ERVCS under MBLOCA

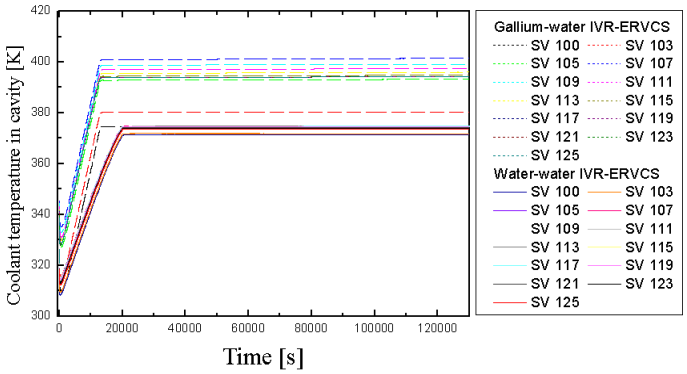

Fig. 4 Coolant temperature distribution in the cavity of the liquid gallium for gallium-water IVR-ERVCS and water for water-water IVR-ERVCS under MBLOCA

gallium level in the cavity and void fraction also do not change as shown in fig. 6 compared to water-water IVR-ERVCS. This point is the main advantage of the gallium-water IVR-ERVCS in terms of the safety margin.

3.2 Heat transfer coefficient

In the MARS-Ga code, the various convective correlations are used according to the heat transfer mode as well as geometry. During the simulation, the gallium-water IVR-ERVCS maintained the single phase liquid convection mode. In this heat transfer mode, Churchill-Chu, McAdams, and Sellars correlations are calculated and the maximum value among these correlations was selected as shown in equation (1)-(3) [6]. In the gallium-water IVR-ERVCS, Churchill-Chu correlation as shown in equation (1) that may be applied over the entire range of Rayleigh number is used. Unlike the gallium-water IVR-ERVCS, the water-water IVR-ERVCS showed the change of the heat transfer mode from the single phase natural convection to subcooled nucleate boiling as shown in

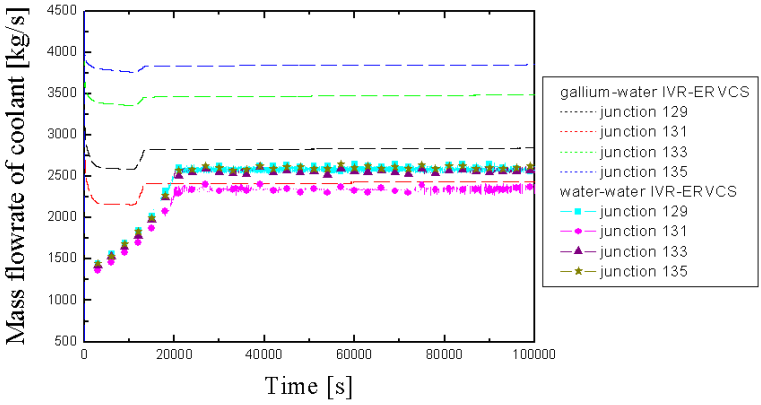

Fig. 5 Mass flowrate of the liquid gallium of the gallium-water IVR-ERVCS and water of the water-water IVR-ERVCS

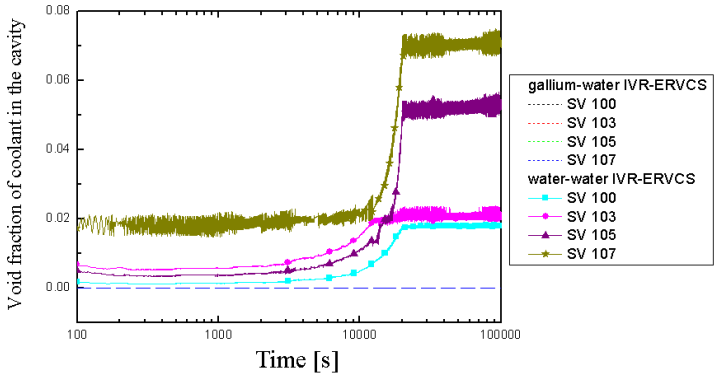

Fig. 6 Void fraction of gallium and water as a coolant in the cavity of the gallium-water and water-water IVR-ERVCS under MBLOCA

$$Nu_L = \left\{ 0.825 + \frac{0.387 Ra_L^{1/6}}{\left[1 + \left(\frac{0.492}{\mathrm{Pr}} \right)^{9/16} \right]^{8/27}} \right\}^2 \quad (1)$$

$$Nu_L = 0.27 Ra_L^{0.25} \quad 10^5 < Ra_L < 10^{10} \quad (2)$$

$$Nu = 4.36 \quad (3)$$

fig. 7 and therefore Churchill-Chu and Chen correlation as shown in equation (1) and (4) are used respectively [7]. The Chen correlation which was a macroscopic convection term plus a microscopic boiling term as shown in equation (4)-(6) is used for the subcooled and saturated nucleate boiling modes.

$$q'' = h_{mac}\left(T_{wall} - T_{spt}\right) + h_{mic}\left(T_{wall} - T_{spt}\right)S \quad (4)$$

$$h_{mac} = 0.023\,\mathrm{Re}_L^{0.8}\,\mathrm{Pr}_L^{0.4}\left(k_L/D\right)F \quad (5)$$

$$h_{mic} = 0.00122\left(\frac{k_f^{0.79}C_{pf}^{0.45}\rho_f^{0.49}}{\sigma^{0.5}\mu_f^{0.29}h_{fg}^{0.24}\rho_g^{0.24}}\right)\left(T_{wall}-T_{spt}\right)^{0.24}\Delta P^{0.75} \quad (6)$$

where, T_{wall} and T_{spt} are wall temperature and steam saturation temperature based on total pressure respectively. k_f, C_{pf}, ρ_f, σ, μ_f, and h_{fg} are thermal conductivity, specific heat, density, surface tension, viscosity, and enthalpy of vaporization of fluid respectively. ρ_g is the density of vapor. Chen correlation chose Dittus-Boelter correlation times a Reynolds number factor, F, for the convection heat transfer part and Forster-Zuber pool boiling correlation [8] times a suppression factor, S, for the boiling heat transfer part. The range of the heat transfer coefficient of liquid gallium is from 2,000 to 21,400 W/m^2·K. Although the heat transfer coefficient of single-phase liquid metal, gallium is lower than boiling heat transfer coefficient of water, the liquid gallium can be maintained at steady state condition because there are no phase change phenomena of liquid gallium compared to water having the rapid change or drop of the heat transfer coefficient after water level decrease.

3.3 Critical Heat Flux

To confirm sufficient margins of CHF (Critical Heat Flux) or no CHF occurrence in the water-water IVR-ERVCS compared to the gallium-water IVR-ERVCS, the higher fluxes up to 3200kW/m^2 of LBLOCA of 9.6" break size of the cold leg without actuation of the safety injection pump were imposed in the heat structures [4-5]. Before considering newly-proposed ERVCS, the simulation of existing IVR-ERVCS of APR 1400 was also performed as a reference study as shown in fig. 2(b). MARS-Ga code uses the 1986 AECL-UO Critical Heat Flux lookup table method by Greoneveld and co-workers [9]. The table is made from the tube data normalized to a tube inside diameter of 0.008m but has factors that are applied to allow its use in other sized tubes or in rod bundles.

$$CHF = CHF_{\text{lookup table}} \times K_{hy}K_{bf}K_{sp}K_{hl}K_{nu}K_{hor}K_{ver} \quad (7)$$

After obtaining CHF from the lookup table, the multiplying factors shown in equation (7) are used to compensate for differences in the heated length geometry, bundle geometry, spacer grid, heat flux profiles, and low flow condition. 7 correction factors such as K_{hy}, K_{bf}, K_{sp}, K_{hl}, K_{nu}, K_{hor}, and K_{ver} are the hydraulic diameter factor, the bundle factor, the grid spacer factor, the heated length factor, the axial flux distribution factor, the horizontal flow factor, and the vertical factor respectively [10]. The value of CHF was

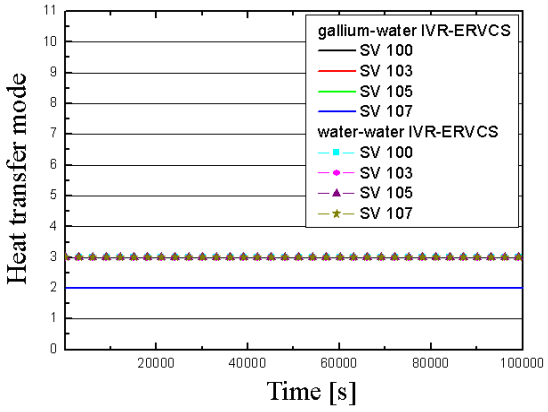

Fig. 7 Heat transfer mode of the gallium-water and water-water IVR-ERVCS under MBLOCA

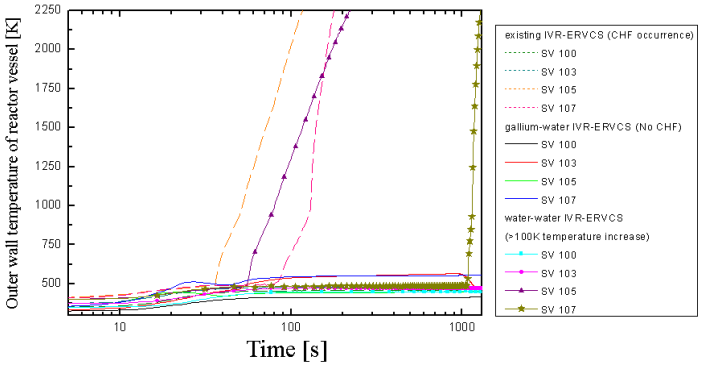

Fig. 8 Wall temperature distribution of outer reactor vessel of the existing, gallium-water and water-water IVR-ERVCS under LBLOCA

calculated in the range of heat transfer mode from the subcooled nucleate boiling to saturated transition boiling. Fig. 8 shows the wall temperature distribution of outer reactor vessel of the existing, gallium-water and water-water IVR-ERVCS under LBLOCA. The mass flowrate of coolants of existing, gallium-water and water-water IVR-ERVCS can be compared as shown in fig. 9. The oscillation of water of existing and water-water IVR-ERVCS can be confirmed unlike gallium-water IVR-ERVCS. Because liquid gallium has a high boiling point, there are no phase change phenomena and therefore sudden changes of the temperature and void fraction do not occur compared to the existing and water-water IVR-ERVCS as shown in fig. 8 and 10. To check the simulation process for predicting the CHF, the heat transfer mode change of MARS-Gs code was checked. With increasing power, the wall temperature of reactor vessel became over 100 K higher than saturated temperature and then the heat transfer mode was changed from nucleate boiling to subcooled film boiling as shown in fig. 11. At that moment, the void fraction and the water temperature are too low and the calculated CHF data by Greoneveld et al. (1986) is higher than given heat flux

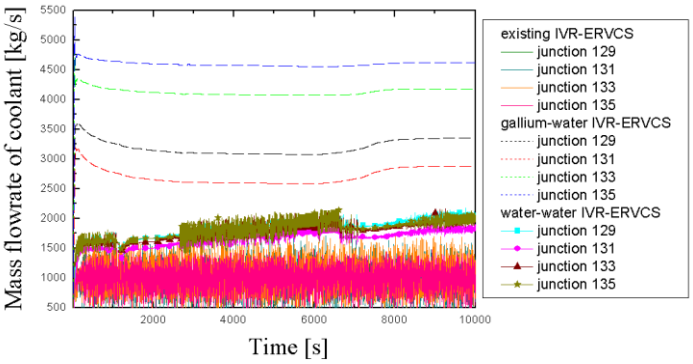

Fig. 9 Mass flowrate of water of the existing IVR-ERVCS, liquid gallium of the gallium-water IVR-ERVCS and water of the water-water IVR-ERVCS

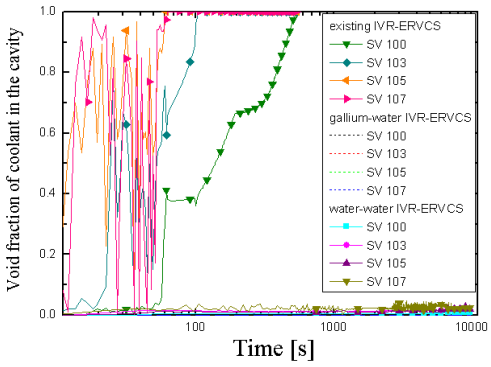

Fig. 10 Void fraction of a coolant in the cavity of the existing, gallium-water and water-water IVR-ERVCS under LBLOCA

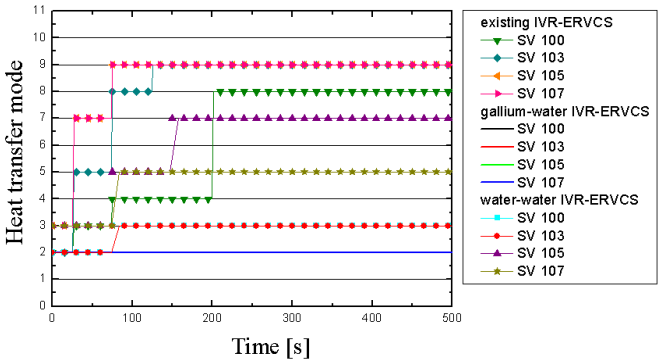

Fig. 11 Heat transfer mode of the existing, gallium-water and water-water IVR-ERVCS under LBLOCA

(~3200kW/m^2) in the subcooled transition boiling mode. In other words, the reason of the sudden change of the wall temperature in the water-water IVR-ERVCS is not that the maximum heat flux is over the calculated CHF data by Greoneveld et al. but the existing IVR-ERVCS shows this trend that the heat transfer mode was changed because the wall temperature is over the 100 K compared to the saturated temperature by following up the flow chart of CHF module in the code. Changing the heat transfer mode, the heat transfer coefficient was suddenly dropped and therefore the increase of wall temperature occurred according to the heat balance in MARS-Ga code. In gallium-water IVR-ERVCS, there were no temperature increases which mean no CHF occurrence or sufficient CHF margin with certain as we expected.

4. Conclusions

For the investigation on the feasibility of the gallium-water IVR-ERVCS based on Park and Bang (2013) [6], numerical simulation for severe accident in APR 1400 using MARS-Ga code as the system analysis code was performed. The gallium-water IVR-ERVCS consists of the liquid metal and water in terms of coolants. The decay heat generated in corium is transferred to liquid metal, gallium through the reactor pressure vessel and then removed from the water pool as an ultimate heat sink. In this research, the configuration for numerical simulation is the side cooling concept that two fluids (liquid gallium and water) were separated by the block structure like so-called liquid metal catcher. Compared to the existing system, the block system was added instead of the cavity wall. To analyze the gallium-water IVR-ERVCS, the MARS-Ga code with the gallium properties is used. The base geometry referred to the APR 1400 and CFD geometry of Park and Bang (2013) [6]. The main consequence of the simulations is the confirmation of heat removal without CHF occurrence from the gallium-water IVR-ERVCS as long as the liquid phase can be maintained in the water pool. The maximum temperature of the liquid gallium is about 402.15 K (129℃) and this result shows that the liquid gallium has the potential to apply IVR-ERVCS as a coolant. Although the heat transfer performance of single-phase liquid gallium is lower than that of boiling water in aspect of the heat transfer coefficient at the initial stage, no phase change phenomena of liquid gallium is the advantage of liquid gallium in terms of CHF margin. It means that the gallium-water IVR-ERVCS can provide the stable and reliable cooling capability at severe accidents in nuclear power plants. To solve the limitation of the existing IVR-ERVCS on the CHF and ensure the sufficient thermal margin, it is analyzed that the gallium-water IVR-ERVCS can be a successful strategy mitigating severe accidents for higher power-capacity nuclear power plants.

REFERENCES

[1] Park, S.D., Bang, I.C., Feasibility of flooding the reactor cavity with liquid gallium coolant for IVR-ERVC strategy, Nuclear Engineering and Design, Vol.258, pp.13-18, 2013.
[2] D.A. Young, “A soft-sphere model for liquid metals”, University of California, Livermore, California, 1977.
[3] Kang, S., Ha, K.S., Kim, H.T., Kim, J.H., Bang, I.C., An experimental study on natural convection heat transfer of

liquid gallium in a rectangular loop, International Journal of Heat and Mass Transfer, Vol.66, pp. 192-199, 2013.
[4] park, R.J., Kim, S.B., Kim, H.D., Detailed analysis of in-vessel melt progression in the LOCA of the KSNP using the SCDAP/RELAP5, Proceedings of the Korean Nuclear Society Spring Meeting, May 27-28, 2004, Gyeongju, Korea.
[5] Kim, S.B., Kim, H.D., Koo, K.M., Park, R.J., Hong, S.W., Cho, Y.R., Kim, J.T., Ha, K.S., Kang, K.H., Kim, H.Y., Optimization of the severe accident management strategy for domestic plants and validation experiments, Korea Atomic Energy Research Institute, KAERI/RR-2528, 2004.
[6] S.W. Churchill, H.H.S. Chu, Correlating equations for laminar and turbulent free convection from a vertical plate, International Journal of Heat Mass Transfer, Vol.18, pp. 1323-1329, 1975.
[7] J.C. Chen, A correlation for boiling heat transfer to saturated fluids in convective flow, Process Design and Development, Vol.5, pp. 322-327, 1966.
[8] H.K. Forster, N. Zuber, Dynamics of vapor bubbles and boiling heat transfer, AIChE Journal, Vol. 1, pp. 531-535, 1955.
[9] D.C. Groeneveld, S.C. Cheng, T. Doan, AECL-UO Critical heat flux lookup table, Heat transfer engineering, Vol.7, pp. 46-62, 1986.
[10] Hwang, J.S., Kim, J.W., Nam, H.U., Park, G.C., Assessment of mars code for predicting critical heat flux under heaving conditions, Nuclear Technology, Vol.176, pp. 260-273, 2010.